Modeling motor neuron resilience in ALS using stem cells

Ilary Allodi[1], Jik Nijssen[1], Julio Aguila Benitez[1], Gillian Bonvicini[1], Ming Cao[1], and Eva Hedlund[1]

[1]*Department of Neuroscience, Karolinska Institutet, Stockholm, Sweden*

To whom correspondence should be addressed: Eva Hedlund at eva.hedlund@ki.se

Running title: Modeling motor neuron resilience in ALS

SUMMARY

Oculomotor neurons, which regulate eye movement, are resilient to degeneration in the lethal motor neuron disease amyotrophic lateral sclerosis (ALS). It would be highly advantageous if motor neuron resilience could be modeled *in vitro*. Towards this goal, we generated a high proportion of oculomotor neurons from mouse embryonic stem cells through temporal overexpression of Phox2a in neuronal progenitors. We demonstrate, using immunocytochemistry and RNA sequencing, that *in vitro* generated neurons are *bona fide* oculomotor neurons based on their similarity to their *in vivo* counterpart in rodent and man. We also show that *in vitro* generated oculomotor neurons display a robust activation of survival-promoting Akt signaling and are more resilient to the ALS-like toxicity of kainic acid than spinal motor neurons. Thus, we can generate *bona fide* oculomotor neurons *in vitro* which display a resilience similar to that seen *in vivo*.

INTRODUCTION

Amyotrophic lateral sclerosis (ALS) is characterized by a loss of motor neurons in cortex, brain stem and spinal cord with subsequent spasticity, muscle atrophy and paralysis. Motor neurons innervating the extraocular muscles, including the oculomotor, trochlear and abducens nuclei, are however relatively resistant to degeneration in ALS (Comley et al., 2016; Gizzi et al., 1992; Nijssen et al., 2017; Nimchinsky et al., 2000). This resilience has been attributed to cell intrinsic properties (Allodi et al., 2016; Brockington et al., 2013; Comley et al., 2015; Hedlund et al., 2010; Kaplan et al., 2014). It would be highly advantageous if differential motor neuron vulnerability could be modeled *in vitro*. This could aid in the identification of gene targets responsible for oculomotor neuron resilience. However, it is not self-evident that *in vitro* generated oculomotor neurons would be more resistant to

degeneration in culture than spinal motor neurons, as multiple cell types contribute to motor neuron degeneration in ALS, including e.g. astrocytes (Yamanaka et al., 2008), microglia (Boillee et al., 2006), oligodendrocytes (Kang et al., 2013) and may play a role in selective vulnerability.

During development, distinct neuronal populations are defined through diffusible morphogens with restricted temporal and spatial patterns and subsequent activation of distinct intrinsic transcription factor programs. These programs can be mimicked to specify different CNS regions and neuronal populations from stem cells *in vitro*. When mouse embryonic stem cells (mESCs) are exposed to Shh (sonic hedgehog) signaling and retinoic acid, which ventralize and caudalize the CNS during development, spinal motor neurons constitute 15-30% of the cells in culture, and interneurons the large remainder (Allodi and Hedlund, 2014; Wichterle et al., 2002). Oculomotor neurons constitute only 1% of the cells in the midbrain and thus patterning mESC cultures with Fgf8 and Shh to direct cultures towards a midbrain/hindbrain fate (Allodi and Hedlund, 2014; Hedlund et al., 2008) results in cultures with too few oculomotor neurons to allow for any quantitative analysis. However, when combining morphogens with overexpression of the intrinsic determinant Phox2a in neural precursors a large proportion of Islet1/2+ brain stem motor neurons can be generated (Mong et al., 2014). However, the exact identity of motor neurons generated this way has not been previously demonstrated and it is currently unclear if these are indeed oculomotor neurons or rather a mix of brain stem motor neurons, including for example trigeminal and facial motor neurons.

Towards the goal of developing stem cell-based *in vitro* models of differential vulnerability we generated cultures with a high proportion of oculomotor neurons through temporal overexpression of Phox2a in mESC-derived neuronal progenitors and compared these to mESC-derived spinal motor neurons. Careful characterization of these distinct motor neuron populations using immunocytochemistry and RNA sequencing demonstrated that mESC-derived oculomotor neurons were highly similar to their *in vivo* counterpart in both rodent and man. Finally, we exposed these to ALS-like conditions using kainic acid and demonstrated that oculomotor neurons were more resilient than spinal motor neurons. Thus, we can generate *bona fide* oculomotor neurons *in vitro* which display a resilience similar to that seen *in vivo*.

RESULTS

Bona fide oculomotor neurons can be generated from mESCs

To characterize the specific identity of brain stem motor neurons generated in culture and compare their properties to spinal motor neurons, we generated neurons from mESCs. Spinal motor neurons were derived by adding 100 nM retinoic acid and the smoothened agonist SAG to the culture for five days. Brain stem motor neurons were specified by overexpressing Phox2a under the nestin enhancer and patterning the culture with Fgf8 and SAG for five days (Figure 1A). Immunocytochemical analysis demonstrated that spinal motor neurons expressed the transcription factors Islet1/2 and Hb9 (Mnx1) (64.1±5.2% Islet1/2+Hb9+ cells, mean±SEM, n=4) (Figure 1B, D, E). Phox2a-overexpressing motor neurons appeared to be of an oculomotor identity as these cells expressed Islet1/2 but lacked Hb9 (6.3±1.3% Islet1/2+Hb9+ cells, mean±SEM, n=4), which is present in all cranial motor neuron nuclei except the oculomotor nucleus (Figure 1C, D, F, G). From hereon we therefore refer to the brain stem motor neurons as oculomotor neurons. In oculomotor neuron cultures 47.5±5.9% (mean±SEM, n=4) of βIII-tubulin+ cells were Islet1/2+ and 62±5.2% (mean±SEM, n=4) of the Islet1/2+ cells were Phox2a+, which demonstrates that 25% of all neurons generated were oculomotor neurons (Figure 1G). To confirm the identity of the cells generated we sorted the motor neurons based on GFP expression using FACS. For this purpose we used a Hb9-GFP mESC line to select for spinal motor neurons and an Islet-GFP::NesEPhox2a mESCs line for the purification of oculomotor neurons (Figure 1a and Figure S1A-D). PolyA-based RNA sequencing of the sorted fractions revealed a similar number of detected genes for both lines (RPKM > 0.1 OMN 13941±293.5 and SC MN 14660.3±304.1; RPKM > 1 OMN 10507±296 and SC MN 10914.3±362.7 mean ± SEM, t test for RPKM > 0.1 P=0.1196, t test for RPKM > 1 P=0.4047, Figure S1E).

Sorted oculomotor neurons clustered closely together in the principal component analysis (PCA) and were separated from spinal motor neurons along the fourth principal component (Figure 1H). Hierarchical clustering of the 1,017 genes that were differentially expressed between oculomotor neurons and spinal motor neurons at an adjusted P value <0.05 demonstrated that each group is defined by a specific set of markers, with a majority of genes being more highly expressed in spinal motor neurons (Figure 1I, Table S1). Analysis of Hox mRNAs clearly demonstrated the more caudal nature of spinal motor neurons compared to oculomotor neurons (Figure S1F). The oculomotor neurons and spinal motor neurons clustered separately based on known marker gene expression e.g. *Phox2a*, *Phox2b*, *Tbx20* and *Rgs4* for oculomotor neurons and *Olig1/2*, *Hb9* and *Lhx1/3* for spinal motor

neurons. Oculomotor neuron cultures were also devoid of noradrenergic neuron markers *NET* and *Th* (Figure 1J).

Using the top 100 differentially expressed genes (DEGs) between our *in vitro* generated oculomotor neurons and spinal motor neurons, we could separate a published microarray data set (Mazzoni et al., 2013) on *in vitro* generated brain stem and spinal motor neurons (Figure S1G). Importantly, we could also use the 100 top DEGs between our oculomotor and spinal motor neurons to separate microarray data originating from mouse oculomotor and spinal motor neurons isolated from P7 mice (Kaplan et al., 2014) (Figure 1K) and from adult rats (Hedlund et al., 2010) (Figure 1L). Thus, our *in vitro* generated motor neuron subpopulations closely resemble their *in vivo* counterparts.

To further delineate the nature of our *in vitro* culture systems, we set out to identify gene clusters regulated in groups of samples in an unbiased way. Here we analyzed all GFP-positive (Hb9+ for spinal and Islet1+ for oculomotor) and -negative fractions from both spinal- and midbrain-specified cultures using PAGODA (Fan et al., 2016). This analysis revealed gene sets enriched in the spinal and oculomotor cultures (GFP+ and GFP- samples), as well as in the motor neuron groups specifically (GFP+) (Figure 1M,N, Table S2). Of the oculomotor-enriched genes found with DESeq2, a subset was enriched in all midbrain-specified cultures (GFP+ and GFP- cells), such as *Phox2a* and Engrailed1 (*En1*). *Fgf10*, known to be expressed in the developing midbrain, including the oculomotor nucleus (Hattori et al., 1997) and Fgf15, with known enrichment in midbrain and rhombomere 1 (Partanen, 2007) were also enriched in our midbrain-specified cultures (Figure 1M). The genes that were highly enriched specifically in oculomotor neurons (GFP+) included *Eya1*, *Eya2*, *Tbx20* and *Phox2b* (Figure 1M). Vice versa, of the genes found to be differentially expressed in spinal motor neurons versus oculomotor neurons with DESeq2, a subset was enriched in all samples of the spinal-specified cultures versus the midbrain-specified cultures. This included for example Hox genes which regulate positional identity e.g. *Hoxc4*, *Hoxd4*, *Hoxa5*, *Hoxb5*, *Hoxb6*, *Hoxb8* and *Hoxd8,* as well as spinal V1 interneuron markers *Sp8* and *Prdm8* . Another subset was found to be highly specific for only the spinal spinal motor neurons, such as *Mnx1* (Hb9) and *Lhx1* (Figure 1N).

Different axon guidance-related genes are expressed by oculomotor and spinal cord motor neurons during development (Bjorke et al., 2016; Gutekunst and Gross, 2014; Stark et al., 2015; Wang et al., 2011). Thus, to further characterize the *in vitro* generated oculomotor neurons, we analyzed their mRNA expression of morphological markers that are important for axon guidance. We found that oculomotor neurons were enriched in *Plxna4, Sema6d*,

Cdh6, *Cdh12*, while spinal motor neurons were enriched for *Epha3, Ephx4, Sema4a* and *Sema5b* (Figure S2A). Analysis of human oculomotor neurons and spinal motor neurons isolated from *post mortem* tissues (Table S3) using laser capture microdissection coupled with RNA sequencing (LCM-seq) (Nichterwitz et al., 2016), showed that also human oculomotor neurons were preferential in *SEMA6D* and *PLXNA4* (Figure S2B). Thus, our *in vitro* generated oculomotor neurons have characteristics distinct from spinal motor neurons regarding genes that govern axon guidance and this is conserved across species.

In conclusion, we have generated a high proportion of *bona fide* oculomotor neurons *in vitro* that can be utilized to understand their normal function as well as resilience to degeneration in motor neuron diseases.

Stem cell-derived oculomotor neurons are relatively resistant to excitotoxicity

To investigate if *in vitro* generated oculomotor neurons are relatively resistant to ALS-like toxicity similarly to their *in vivo* counterparts, we used kainic acid which is a neuro-excitatory amino acid that acts by activating glutamate receptors. Glutamate excitotoxicity is thought to be a downstream event in motor neuron degeneration in ALS and thus considered appropriate to model this disease. First, we evaluated the mRNA levels of glutamate ionotropic receptors in our cultures to ensure that generated neurons could respond to kainic acid. mRNA sequencing data of sorted motor neurons demonstrated that oculomotor neurons and spinal motor neurons expressed similar levels of AMPA, NMDA and kainate receptor subunits (Figure 2a). Grik5 was the subunit expressed at highest level (Figure 2A) and it was also detectable at the protein level in both oculomotor (Figure 2B) and spinal (Figure 2C) motor neurons. Thus, both motor neuron types should respond to kainic acid. Exposure of the cultures to kainic acid for one week demonstrated that oculomotor neurons were more resilient to the elicited long-term excitotoxicity than spinal motor neurons (ANOVA, $*P < 0.05$, Figure 2D-F).

Stem cell-derived cultures are not temporally restricted in a precise way. Cultures that contain post mitotic neurons will also harbor neuronal progenitors that later on are specified into neurons. It can thus be challenging to distinguish survival from renewal in a stem cell-based *in vitro* system. We therefore analyzed the turn-over rate in our cultures by pulsing these with BrdU. Analysis of the number of BrdU+ Islet1/2+ neurons demonstrated that a significantly higher number of motor neurons were generated over time in the spinal motor neuron cultures compared to the oculomotor neuron cultures (Figure S1H). Consequently, the resilience of oculomotor neurons should be considered even more pronounced as these

cultures had a comparatively low turn-over rate. Using Sholl analysis to evaluate arborization complexity it also became evident that oculomotor neuron processes remained morphologically unaffected by kainic acid (Figure 2G-I). In support of this, oculomotor neurons had a high expression of β-catenin after kainate treatment compared to spinal motor neurons, with the expression being preferential to processes (Figure 2F-H).

As axonal fragmentation and degeneration is seen early on in motor neurons in ALS, our data clearly demonstrates that oculomotor neurons cope well under conditions of excitotoxicity.

In conclusion, *in vitro* generated oculomotor neurons are highly resilient to ALS-like excitotoxicity. Thus, the pattern of selective motor neuron vulnerability seen *in vivo* can be replicated *in vitro*.

Oculomotor neurons have high levels of calcium buffering proteins and Akt signaling which could contribute to resilience

To explain the resilience of *in vitro* generated oculomotor neurons to excitotoxicity we conducted a directed comparative analysis of the RNA sequencing data from purified oculomotor neurons versus spinal motor neurons. It has been suggested that preferential expression of calcium binding proteins in oculomotor neurons plays a role in their resilience (Comley et al., 2015; Van Den Bosch et al., 2002). We focused on transcripts with implications in calcium handling. Our analysis demonstrated that Cald1, Esyt1, Camk2a and Hpca11 were preferentially expressed in oculomotor neurons (Figure S3A). Esyt1 protein levels were also preferential to oculomotor neurons and unaffected by kainic acid treatment (Figure S3B-D). This could render oculomotor neurons with an increased capacity to buffer Ca^{2+} intracellularly.

We have previously shown that Akt signaling is important in motor neuron resilience towards ALS after IGF-2 treatment (Allodi et al., 2016). We therefore analyzed our RNA sequencing data from sorted oculomotor and spinal motor neurons for Akt signaling effectors which could aid in explaining the relative resilience of oculomotor neurons *in vitro*. This analysis demonstrated an elevated expression of Akt1 and Akt3 in oculomotor neurons compared to spinal motor neurons (adjusted $P < 0.05$, Figure 3A). To evaluate if our *in vitro* data has relevance for human oculomotor neuron resistance we conducted RNA sequencing on human oculomotor and spinal motor neurons isolated by laser capture microdissection (LCM-seq) (Nichterwitz et al., 2018; Nichterwitz et al., 2016). This analysis clearly demonstrated that also human oculomotor neurons have a preferential activation of the

PI3K-Akt signaling pathway compared to human spinal motor neurons as demonstrated by their higher expression of AKT1 and AKT3 (adjusted $P < 0.05$, Figure 3B). Consistent with our RNA sequencing findings, immunocytochemistry against pAkt and quantification of fluorescent intensities in Islet1/2^{+} oculomotor and spinal motor neurons derived from mESCs demonstrated that oculomotor neurons had higher levels of pAkt protein than spinal motor neurons (Figure 3C-E). These levels were maintained after excitotoxicity elicited by kainic acid (2-way ANOVA, *** $P < 0.0001$, Figure 3E).

To further validate this pathway in oculomotor neuron resistance we analyzed the protein levels of activated β-catenin (non-phosphorylated), a down-stream effector of Akt signaling, using immunocytochemistry. The semi-quantitative analysis demonstrated that oculomotor neurons had elevated levels of β-catenin compared to spinal cord motor neurons (2-way ANOVA, *** $P < 0.0001$, Figure 3F). β-catenin expression was maintained at relatively high levels in oculomotor neurons compared to spinal motor neurons also during kainate toxicity, with expression preferentially localized to processes. Expression of CTNNB1 (β-catenin) was also relatively higher in human oculomotor neurons compared spinal motor neurons that were isolated from human fresh frozen tissue (Figure 3G).

Our data thus indicate that Akt signaling, which is a known survival pathway, could contribute to oculomotor neuron resistance in man and mouse *in vivo* as well as in a dish.

DISCUSSION

In ALS, motor neuron subpopulations show differential vulnerability to degeneration. In particular, cranial motor neurons of the oculomotor, trochlear and abducens (cranial nerves 3, 4 and 6), which innervate the extraocular muscles around the eyes are highly resistant throughout disease progression. In our study we demonstrate that a high proportion of *bona fide* oculomotor neurons can be generated from mESC through temporal over-expression of Phox2a, and that these are relatively resilient to ALS-like toxicity.

Oculomotor neurons are generated in the ventral midbrain through the specification by Shh (secreted from the floor plate and the notochord) Fgf8 and Wnts (both secreted by and around the isthmic organiser). These morphogens in turn regulate transcription factors that influence differentiation of ventral midbrain neurons, including oculomotor neurons, dopamine neurons, red nucleus neurons and GABA-positive interneurons (reviewed in (Nijssen et al., 2017)). Oculomotor neurons are specified by the transcription factors Phox2a, Phox2b and Lmx1b (Deng et al., 2011; Pattyn et al., 1997). Phox2a is required to drive

oculomotor neuron fate as demonstrated by the lack of both oculomotor and trochlear nuclei in Phox2a knockout mice (Pattyn et al., 1997). Phox2a is also sufficient to generate a complete oculomotor complex as shown by studies in chick (Hasan et al., 2010; Pattyn et al., 1997). Phox2b on the other hand is sufficient to induce ectopic generation of oculomotor neurons in the spinal cord, but it is not required to induce oculomotor neuron specification in the midbrain (Dubreuil et al., 2000; Pattyn et al., 1997). *In vitro* studies have shown that; *i)* mESCs can be directly programmed into cranial neurons using the proneuronal gene *Ngn2*, in combination with *Islet1* and *Phox2a* (Mazzoni et al., 2013), and that *ii)* over-expression of either Phox2a or Phox2b alone in mESC-derived neural progenitors exposed to Shh and Fgf8 can promote a midbrain/hindbrain motor neuron fate (Mong et al., 2014). However, while it was demonstrated that cranial motor neurons were generated *in vitro* it was never previously determined if oculomotor neurons were specifically produced.

Here, we show that Phox2a overexpression in neural progenitors in combination with patterning using Fgf8 and Shh results in the generation of 50% Islet+ neurons of which more than half were Phox2a+. The transcriptome and proteome of oculomotor neurons is distinct from other motor neurons (reviewed in (Nijssen et al., 2017)). Notably, oculomotor neurons can be distinguished by their lack of the transcription factor Hb9, which defines other somatic motor neurons. As the vast majority of Islet+ cells in our midbrain cultures lacked Hb9 we conclude that the Phox2a+ cells generated were indeed oculomotor neurons and that Phox2a overexpression is sufficient to induce an oculomotor fate from stem cells *in vitro*. This conclusion was further supported by our RNA sequencing experiments on purified oculomotor and spinal motor neuron cultures and our bioinformatics cross-comparison with other *in vitro* and *in vivo* data set from rodent and man (Brockington et al., 2013; Hedlund et al., 2010; Kaplan et al., 2014), which confirmed that the oculomotor neurons we generated were similar to their *in vivo* counterpart and thus we can generate *bona fide* oculomotor neurons.

Furthermore, our analysis of axon guidance molecules demonstrated differential expression of distinct morphological markers in oculomotor and spinal motor neurons. Importantly our RNA sequencing analysis of human motor neurons analyzed from post mortem material showed that the distinction in these morphological markers were conserved across species.

Multiple studies have demonstrated that differential motor neuron vulnerability appears to be regulated by cell intrinsic differences in gene expression (Allodi et al., 2016; Brockington

et al., 2013; Hedlund et al., 2010). We therefore hypothesized that *in vitro* generated oculomotor neurons would be more resilient to ALS-like toxicity than spinal motor neurons. Indeed, our experiments on neuronal vulnerability clearly demonstrated that oculomotor neurons were more resistant to the ALS-like toxicity elicited by kainic acid than spinal motor neurons. Furthermore, the fact that oculomotor neuron processes remained intact indicates that these cells were indeed highly resilient as axonal degeneration is an early sign of pathology in ALS.

It has been shown that oculomotor neurons have a higher calcium buffering capacity than other motor neuron groups (Vanselow and Keller, 2000), which could render the cells more resilient to excitotoxic insuts. Our finding that several transcripts with implications for calcium handling were preferentially expressed in stem cell derived oculomotor neurons and also in oculomotor neurons in man were thus very compelling and consistent with their resilience. Esyt1, for example, is an ER integral membrane protein which presents a cytosolic synaptotagmin-like domain that can bind organelle membranes and a C2 domain able to bind the plasma membrane. These interactions are involved in exchange of lipids and vescicles but also in the ER control of Ca^{2+} homeostasis. Thus, ER-plasma membrane junctions can control Ca^{2+} release from ER in response to extracellular Ca^{2+} levels (Giordano et al., 2013), an event that could have a beneficial effect during excitotoxicity.

Furthermore, we have previously shown that Akt signaling plays an important role in induced resistance in vulnerable motor neurons (Allodi et al., 2016). We now demonstrate that Akt signaling is more highly activated in resistant oculomotor neurons *in vitro* as well as *in vivo* in human oculomotor neurons. This would indicate that oculomotor neurons preferentially activate a cell intrinsic survival program. In conclusion, we have demonstrated that *bona fide* oculomotor neurons can be generated from stem cells *in vitro.* We also show that these neurons are relatively resilient to ALS-like toxicity. This novel finding enables modeling of neuronal resistance and susceptibility in ALS *in vitro* which could further elucidate mechanisms that could be highly advantageous to activate *in vivo* to rescue vulnerable motor neurons from degeneration.

EXPERIMENTAL PROCEDURES

Ethics Statement

All work was carried according to the Code of Ethics of the World Medical Association (Declaration of Helsinki). Animal procedures were approved by the Swedish animal ethics review board (Stockholm Norra Djurförsöksetiska Nämnd). Human CNS samples were obtained from the Netherlands Brain Bank (NBB, www.brainbank.nl) and the National Disease Research Interchange (NDRI, www.ndriresource.org) with the written informed consent from the donors or next of kin.

Generation of mESC lines and specification into oculomotor and spinal motor neurons

Three different mouse ESC lines were used in this study: E14.1 (ATCC), Hb9-GFP (gift from Dr. S. Thams, Karolinska Institutet) and Islet1-GFP (gift from Prof. S. Pfaff, UCSD). To increase oculomotor neuron differentiation efficiency E14.1/NesEPhox2A and Islet1-GFP/NesEPhox2A ESC lines were generated by Lipofectamine (Invitrogen) transduction, NesEPhox2A construct was a gift from Prof. J. Ericson, Karolinska Institutet. Specification of mESCs into spinal motor neurons was conducted by exposing embryo bodies to the Smoothened Agonist SAG (500 nM, #364590-63-6 Calbiochem) and retinoic acid (RA, 100 nM, #302-79-4 Calbiochem) for 5 days, while oculomotor neurons were patterned by SAG (250 nM) and Fgf8 (100 ng/ml, #423-F8 R&D systems) for 5 days. Media containing morphogens was replaced daily. EB dissociation and motor neuron culture maintenance was carried out as previously described (Wichterle et al., 2002).

Fluorescent-Activated Cell Sorting and RNA sequencing of stem-cell derived neurons

Islet1-GFP/NesEPhox2A and Hb9-GFP ESCs were differentiated in oculomotor and spinal motor neurons respectively. GFP+ motor neurons were sorted, and positive and negative fractions were collected for mRNA-sequencing or plated for subsequent immunocytochemistry analysis. FACS was performed using a 100 µm nozzle, a sheath pressure of 15-25 pounds per square inch (psi) and an acquisition rate of 1,000-2,000 events/second (Hedlund et al., 2008). $5x10^3$ cells were collected in a 5% Triton-X-100 (Sigma-Aldrich) in water solution and then prepared for RNA-seq as previously described (Nichterwitz et al., 2016). Samples were sequenced on Illumina HiSeq2000 and HiSeq2500 platforms with readlengths of 43 and 51 bp, respectively.

Laser capture microdissection and RNA sequencing of human motor neurons

Laser capture microdissection of motor neurons from human post mortem tissues coupled with RNA sequencing, LCM-seq, was performed as previously described (Nichterwitz et al.,

2018; Nichterwitz et al., 2016). Briefly, midbrain and spinal cord tissues were sectioned at 10 µm thickness and stained using a quick histological Nissl stain based on the Arcturus Histogene Staining Kit protocol. Slides were then placed under a Leica DM6000R/CTR6500 microscope and captured using the Leica LMD7000 system. Pools of approximately 50-120 cells were collected and directly lysed in 5µl of 0.2% triton X-100 (Sigma-Aldrich) with RNAse inhibitor (1.5U, Takara). After lysis samples were immediately frozen on dry ice until further processing.

RNA-seq data processing

Reads from cell culture samples were mapped to the mouse mm10 reference genome with HISAT2 (Kim et al., 2015), using the publicly available infrastructure (available at usegalaxy.org) on the main Galaxy server (Afgan et al., 2016). Human LCM samples were mapped to hg38/GRCh38 using the same infrastructure and algorithm. Transcript level counts were assigned using the GenomicAlignments package in R (version 1.8.4) (Lawrence et al., 2013) with the function summarizeOverlaps, mode set to 'union'. For visualization of expression data, RPKM data were calculated using total exon gene lengths derived from the Ensembl mm10 genome annotation version GRCm38.87 for mouse and the Ensembl hg38 genome annotation version GRCh38.81 for human. After mapping, exclusion criteria were: < 500.000 mapped reads or a Spearman correlation to other samples < 0.4.

Differential gene expression analysis was performed with the DESeq2 package in R (version 1.12.4) (Love et al., 2014). Only genes with counts in at least 4 samples were considered for further analysis. No fold change cutoff was implemented and multiple testing correction was performed using the Benjamini & Hochberg correction with an FDR set to 10%. Adjusted p-values < 0.05 were considered significant. Pathway And Gene set OverDispersion Analysis (PAGODA) was run using the SCDE package in R (Fan et al., 2016). All heatmaps were generated in R with either no clustering or *euclidean distance* where appropriate.

Immunocytochemistry and immunohistochemistry

Coverslips were fixed in 4% paraformaldehyde in 0.1M phosphate buffer (4% PFA) for 20 minutes, washed with PBS and then blocked with blocking solution composed of 10% normal donkey serum or normal goat serum (both from Thermo Fisher Scientific Inc.) and 0.1% Triton-X-100 in PBS for one hour at room temperature. Coverslips were incubated overnight with primary antibodies in blocking solution at 4˚C and then incubated with Alexa

Fluorophore 488, 568 or 647 secondary antibodies (Invitrogen) one hour at room temperature. The following primary antibodies were used: NF200 (1:1000, #AB5539 Millipore), Tuj1 (1:1000, MRB-435P Covance), Hb9 (1:10, #81.5C10 DSHB), Islet1 (1:500, #ab20670 abcam; 1:100, #40.2D6 DSHB), Phox2A (1:1000, gift of Prof JF Brunet), GFP (1:1000, #ab13970 abcam), phospho-AKT (Ser473) (1:50, #3787 Cell Signaling), activated beta-catenin (1:1000, #05-665 Millipore), alpha-catenin (1:1000, #AB153721 AbCam), ESYT1 (1:100, #HPA016858), BrdU (1:10, #G3G4 DSHB). Hoechst-33342 (Invitrogen) was used as a counterstain. Finally, coverslips were mounted on glass slides using Mowiol 4-88 mounting media (Calbiochem). For immunocytochemistry semi-quantifications and BrdU quantifications at least 3 experiments per condition were counted in technical duplicates. Between 10 and 12 random areas were analyzed per coverslip by blind researcher. For validation of ESYT1 antibody, immunohistochemistry was performed on adult mouse tissue at midbrain and spinal cord levels. Briefly, mice were transcardially perfused with PBS and then with 4% PFA. Brains and spinal cords were dissected and post-fixed for 3 and 1 hour respectively in 4% PFA. Tissue was then cryoprotected with 30% sucrose and then cut at 30 μm thickness. Immunohistochemistry for ESYT1 was performed as indicated above.

ALS-Like toxicity and motor neuron survival

Oculomotor and spinal motor neurons were cultured for 5 days and then exposed to kainic acid. Three concentrations of kainic acid were tested, 20, 50 and 100 μM. A concentration of 20 μM was found sufficient to induce consistent motor neuron death also when motor neurons were cultured on astrocytes. Kainate toxicity was induced for 7 days. Quantifications were performed blind to the motor neuron population and toxicity condition. Pictures were taken with a Zeiss LSM700 confocal microscope (40x magnification and 1.5 digital zoom) using the ZEN 2010S SP1 software and then further analyzed by ImageJ software. At least four experiments per condition were quantified in technical duplicates. 12 random areas were quantified per each coverslip (at least 130 cells were quantified for each condition). To evaluate proliferation and generation of motor neurons, cultures were exposed to pulses of bromodeoxyuridine (BrdU, #B5002 Sigma) for 24 hours. BrdU was dissolved in Dimethyl Sulfoxide (DMSO, #276855 Sigma) and added to the cultures at a final concentration of 10 μM. After 24 hour exposre to BrdU, cells were washed twice with fresh culture media. Proliferation was assessed at day 0 (D0), day 2 (D2) and day 3 (D3) of the survival protocol and all samples were fixed with 4% PFA at day 7 (D7). Quantifications were performed in triplicates with technical duplicates.

Sholl analysis

Sholl analysis was conducted utilizing a Sholl Analysis plugin for Fiji software. The complexity of OMN arborization was obtained by Sholl analysis (O'Neill et al., 2015)by calculating the average of neurites intersecting defined concentric cycles spaced 25 µm from each other starting from the center of the cell body as a function of distance from soma. Individual OMNs were analyzed after culturing them at lower density (SC MN analysis could not be performed due to their poor survival at lower densities). Several microphotographs were taken at 40x magnification with a Zeiss LSM700 confocal microscope, mounted with Adobe Photoshop software and analyzed with Fiji software. The intersection averages were analyzed by multiple t test.

Statistical Analysis

All statistical analyses were performed with GraphPad software unless otherwise specified. Two-way analysis of variance (ANOVA) was used when taking in account multiple variables and making multiple comparisons, followed by appropriate *post hoc* analysis. Unpaired Student's t test was used to compare two groups. Further details on statistical tests used can be found in figure legends as well as total number of motor neurons counted per experiment. All experiments were performed at least in triplicates with technical duplicates. All results are expressed as mean ± SEM unless otherwise specified.

ACCESSION NUMBERS

The original RNA sequencing data from this study are available at the NCBI Gene Expression Omnibus (GEO, http://www.ncbi.nlm.nih.gov/geo/) under accession number GSE118620 (*in vitro* generated neuron data) and GSE93939 (human LCM-seq data).

SUPPLEMENTAL INFORMATION

Supplemental information consists of three figures, two tables and can be found within this article online at

AUTHOR CONTRIBUTIONS

E.H. conceived the study. E.H and I.A. supervised the project. E.H, I.A, J.N. and J.A.B. designed experiments. IA., J.N., J.A.B., G.B. and M.C. acquired data. IA., J.N., J.A.B., G.B., M.C. and E.H. analyzed data. E.H. wrote the manuscript with the help of I.A. and J.N. All authors edited and gave critical input on the manuscript.

ACKNOWLEDGEMENTS

This work was supported by grants from the Swedish Research Council (2011-2651, 2016-02112); EU Joint Programme for Neurodegenerative Disease (JPND) (529-2014-7500); Ragnar Söderbergs stiftelse (M245/11) and Åhlén-stiftelsen (mA9/h11, mA5/h12, mB8/h13, mB8/h14, mA1/h15, mA1/h16) to E.H. I.A. was supported by a postdoctoral fellowship from the Swedish Society for Medical Research (SSMF) (2015-2017) and J.A.B. is currently supported by a postdoctoral fellowship from SSMF (2017-2019).

CONFLICT OF INTEREST

The authors declare that there are no conflicts of interest.

REFERENCES

Afgan, E., Baker, D., van den Beek, M., Blankenberg, D., Bouvier, D., Cech, M., Chilton, J., Clements, D., Coraor, N., Eberhard, C., et al. (2016). The Galaxy platform for accessible, reproducible and collaborative biomedical analyses: 2016 update. Nucleic Acids Res 44, W3-W10.

Allodi, I., Comley, L., Nichterwitz, S., Nizzardo, M., Simone, C., Benitez, J.A., Cao, M., Corti, S., and Hedlund, E. (2016). Differential neuronal vulnerability identifies IGF-2 as a protective factor in ALS. Sci Rep 6, 25960.

Allodi, I., and Hedlund, E. (2014). Directed midbrain and spinal cord neurogenesis from pluripotent stem cells to model development and disease in a dish. Front Neurosci 8, 109.

Bjorke, B., Shoja-Taheri, F., Kim, M., Robinson, G.E., Fontelonga, T., Kim, K.T., Song, M.R., and Mastick, G.S. (2016). Contralateral migration of oculomotor neurons is regulated by Slit/Robo signaling. Neural Dev 11, 18.

Boillee, S., Yamanaka, K., Lobsiger, C.S., Copeland, N.G., Jenkins, N.A., Kassiotis, G., Kollias, G., and Cleveland, D.W. (2006). Onset and progression in inherited ALS determined by motor neurons and microglia. Science 312, 1389-1392.

Brockington, A., Ning, K., Heath, P.R., Wood, E., Kirby, J., Fusi, N., Lawrence, N., Wharton, S.B., Ince, P.G., and Shaw, P.J. (2013). Unravelling the enigma of selective vulnerability in neurodegeneration: motor neurons resistant to degeneration in ALS show distinct gene expression characteristics and decreased susceptibility to excitotoxicity. Acta Neuropathol 125, 95-109.

Comley, L., Allodi, I., Nichterwitz, S., Nizzardo, M., Simone, C., Corti, S., and Hedlund, E. (2015). Motor neurons with differential vulnerability to degeneration show distinct protein signatures in health and ALS. Neuroscience 291, 216-229.

Comley, L.H., Nijssen, J., Frost-Nylen, J., and Hedlund, E. (2016). Cross-disease comparison of amyotrophic lateral sclerosis and spinal muscular atrophy reveals conservation of selective

vulnerability but differential neuromuscular junction pathology. J Comp Neurol 524, 1424-1442.

Deng, Q., Andersson, E., Hedlund, E., Alekseenko, Z., Coppola, E., Panman, L., Millonig, J.H., Brunet, J.F., Ericson, J., and Perlmann, T. (2011). Specific and integrated roles of Lmx1a, Lmx1b and Phox2a in ventral midbrain development. Development 138, 3399-3408.

Dubreuil, V., Hirsch, M.R., Pattyn, A., Brunet, J.F., and Goridis, C. (2000). The Phox2b transcription factor coordinately regulates neuronal cell cycle exit and identity. Development 127, 5191-5201.

Fan, J., Salathia, N., Liu, R., Kaeser, G.E., Yung, Y.C., Herman, J.L., Kaper, F., Fan, J.B., Zhang, K., Chun, J., et al. (2016). Characterizing transcriptional heterogeneity through pathway and gene set overdispersion analysis. Nat Methods 13, 241-244.

Giordano, F., Saheki, Y., Idevall-Hagren, O., Colombo, S.F., Pirruccello, M., Milosevic, I., Gracheva, E.O., Bagriantsev, S.N., Borgese, N., and De Camilli, P. (2013). PI(4,5)P(2)-dependent and Ca(2+)-regulated ER-PM interactions mediated by the extended synaptotagmins. Cell 153, 1494-1509.

Gizzi, M., DiRocco, A., Sivak, M., and Cohen, B. (1992). Ocular motor function in motor neuron disease. Neurology 42, 1037-1046.

Gutekunst, C.A., and Gross, R.E. (2014). Plexin a4 expression in adult rat cranial nerves. J Chem Neuroanat 61-62, 13-19.

Hasan, K.B., Agarwala, S., and Ragsdale, C.W. (2010). PHOX2A regulation of oculomotor complex nucleogenesis. Development 137, 1205-1213.

Hattori, Y., Yamasaki, M., Konishi, M., and Itoh, N. (1997). Spatially restricted expression of fibroblast growth factor-10 mRNA in the rat brain. Brain Res Mol Brain Res 47, 139-146.

Hedlund, E., Karlsson, M., Osborn, T., Ludwig, W., and Isacson, O. (2010). Global gene expression profiling of somatic motor neuron populations with different vulnerability identify molecules and pathways of degeneration and protection. Brain 133, 2313-2330.

Hedlund, E., Pruszak, J., Lardaro, T., Ludwig, W., Vinuela, A., Kim, K.S., and Isacson, O. (2008). Embryonic stem cell-derived Pitx3-enhanced green fluorescent protein midbrain dopamine neurons survive enrichment by fluorescence-activated cell sorting and function in an animal model of Parkinson's disease. Stem Cells 26, 1526-1536.

Kang, S.H., Li, Y., Fukaya, M., Lorenzini, I., Cleveland, D.W., Ostrow, L.W., Rothstein, J.D., and Bergles, D.E. (2013). Degeneration and impaired regeneration of gray matter oligodendrocytes in amyotrophic lateral sclerosis. Nat Neurosci 16, 571-579.

Kaplan, A., Spiller, K.J., Towne, C., Kanning, K.C., Choe, G.T., Geber, A., Akay, T., Aebischer, P., and Henderson, C.E. (2014). Neuronal matrix metalloproteinase-9 is a determinant of selective neurodegeneration. Neuron 81, 333-348.

Kim, D., Langmead, B., and Salzberg, S.L. (2015). HISAT: a fast spliced aligner with low memory requirements. Nat Methods 12, 357-360.

Lawrence, M., Huber, W., Pages, H., Aboyoun, P., Carlson, M., Gentleman, R., Morgan, M.T., and Carey, V.J. (2013). Software for computing and annotating genomic ranges. PLoS Comput Biol 9, e1003118.

Love, M.I., Huber, W., and Anders, S. (2014). Moderated estimation of fold change and dispersion for RNA-seq data with DESeq2. Genome Biol 15, 550.

Mazzoni, E.O., Mahony, S., Peljto, M., Patel, T., Thornton, S.R., McCuine, S., Reeder, C., Boyer, L.A., Young, R.A., Gifford, D.K., et al. (2013). Saltatory remodeling of Hox chromatin in response to rostrocaudal patterning signals. Nat Neurosci 16, 1191-1198.

Mong, J., Panman, L., Alekseenko, Z., Kee, N., Stanton, L.W., Ericson, J., and Perlmann, T. (2014). Transcription factor-induced lineage programming of noradrenaline and motor neurons from embryonic stem cells. Stem Cells 32, 609-622.

Nichterwitz, S., Benitez, J.A., Hoogstraaten, R., Deng, Q., and Hedlund, E. (2018). LCM-Seq: A Method for Spatial Transcriptomic Profiling Using Laser Capture Microdissection Coupled with PolyA-Based RNA Sequencing. Methods Mol Biol 1649, 95-110.

Nichterwitz, S., Chen, G., Aguila Benitez, J., Yilmaz, M., Storvall, H., Cao, M., Sandberg, R., Deng, Q., and Hedlund, E. (2016). Laser capture microscopy coupled with Smart-seq2 for precise spatial transcriptomic profiling. Nat Commun 7, 12139.

Nijssen, J., Comley, L.H., and Hedlund, E. (2017). Motor neuron vulnerability and resistance in amyotrophic lateral sclerosis. Acta Neuropathol 133, 863-885.

Nimchinsky, E.A., Young, W.G., Yeung, G., Shah, R.A., Gordon, J.W., Bloom, F.E., Morrison, J.H., and Hof, P.R. (2000). Differential vulnerability of oculomotor, facial, and hypoglossal nuclei in G86R superoxide dismutase transgenic mice. J Comp Neurol 416, 112-125.

O'Neill, K.M., Akum, B.F., Dhawan, S.T., Kwon, M., Langhammer, C.G., and Firestein, B.L. (2015). Assessing effects on dendritic arborization using novel Sholl analyses. Front Cell Neurosci 9, 285.

Partanen, J. (2007). FGF signalling pathways in development of the midbrain and anterior hindbrain. J Neurochem 101, 1185-1193.

Pattyn, A., Morin, X., Cremer, H., Goridis, C., and Brunet, J.F. (1997). Expression and interactions of the two closely related homeobox genes Phox2a and Phox2b during neurogenesis. Development 124, 4065-4075.

Stark, D.A., Coffey, N.J., Pancoast, H.R., Arnold, L.L., Walker, J.P., Vallee, J., Robitaille, R., Garcia, M.L., and Cornelison, D.D. (2015). Ephrin-A3 promotes and maintains slow muscle fiber identity during postnatal development and reinnervation. J Cell Biol 211, 1077-1091.

Van Den Bosch, L., Schwaller, B., Vleminckx, V., Meijers, B., Stork, S., Ruehlicke, T., Van Houtte, E., Klaassen, H., Celio, M.R., Missiaen, L., et al. (2002). Protective effect of parvalbumin on excitotoxic motor neuron death. Exp Neurol 174, 150-161.

Vanselow, B.K., and Keller, B.U. (2000). Calcium dynamics and buffering in oculomotor neurones from mouse that are particularly resistant during amyotrophic lateral sclerosis (ALS)-related motoneurone disease. J Physiol 525 Pt 2, 433-445.

Wang, L., Klein, R., Zheng, B., and Marquardt, T. (2011). Anatomical coupling of sensory and motor nerve trajectory via axon tracking. Neuron 71, 263-277.

Wichterle, H., Lieberam, I., Porter, J.A., and Jessell, T.M. (2002). Directed differentiation of embryonic stem cells into motor neurons. Cell 110, 385-397.

Yamanaka, K., Chun, S.J., Boillee, S., Fujimori-Tonou, N., Yamashita, H., Gutmann, D.H., Takahashi, R., Misawa, H., and Cleveland, D.W. (2008). Astrocytes as determinants of disease progression in inherited amyotrophic lateral sclerosis. Nat Neurosci 11, 251-253.

Figure legends

Figure 1. Phox2a overexpression drives the generation of *bona fide* oculomotor neurons from stem cells. (a) Time line depicting in vitro protocols for resistant oculomotor neurons (OMN) and vulnerable spinal motor neuron (SC MN) generation. ESC column reports the four cell lines used in this study. Patterning was performed for 5 days after ESC expansion and EB formation. mRNA-seq coupled with FACS was performed on EB dissociation day (day 9 of the protocol). Survival assay was performed after five days from EB dissociation. (b-c) SC MNs generated from E14.1 ESCs express Hb9, Islet1 and NF200, OMNs generated from E14.1 ESCs over-expressing the transcription factor Phox2a under the Nestin enhancer co-express Islet1 and NF200 in absence of Hb9. Scale bar in c 60 µm. (d) Percentage of Hb9+/Islet1+ cells in SC MN (64.1±5.2%, mean±SEM, n=4) and OMN (6.3±1.3%, mean±SEM) cultures respectively. (For quantification, experiments were run in quadruplicates including two technical replicates per experiment, with at least 120 Islet1+ cells counted per condition). (e) Microphotographs showing Islet1+/Tuj1+ cells in OMN cultures, (f) OMNs also express the specific marker Phox2a as indicated by asterisks. Scale bars in e and g 100 µm. (g) Quantification of Islet1+ over Tuj1+ cells demonstrates that half neuronal population appears to be Islet1+ (47.5±5.9%, mean±SEM, experiments performed in quadruplicates with two technical replicates each, total number of Tuj1+ cells counted: 1325). Quantification of Phox2A+ over Islet1+ cells (experiments performed in quadruplicates with two technical replicates each, total number Islet1+ cells counted: 746) indicates that 62±5.2% (mean±SEM) of the Islet1+ population is also Phox2a+. All quantifications were performed 5 days after EB dissociation (mean ± SEM). (h) PCA of OMN and SC MN samples based on all genes expressed confirmed cell differential identities. mRNA-seq analysis of OMNs and SC MNs isolated by FACS was performed after 5 days of patterning (day 9 of the

protocol). (i) 1,017 differentially expressed genes were found between the two different cell types (adjusted P<0.05). Heatmap shows the top 500 most significant differentially expressed genes by adjusted p-value. (j) Heatmap of expected progenitors and motor neuron transcripts but also OMN and SC MN specific transcripts obtained in the two generated motor neuron populations. (k) Using the top 100 DEGs obtained from our RNAseq analysis we could separate datasets originating from *in vivo* microarray studies on early postnatal (j) and adult (l) rodent OMNs and SC MNs. (m) Venn diagram showing gene sets enriched either in brain stem cultures or OMN-specific as revealed by PAGODA analysis, (n) gene sets preferentially found in spinal cord cultures or MN-specific.

Figure 2. ***In vitro* generated oculomotor neurons are relatively resistant to ALS-like toxicity.** (a) Oculomotor neurons (OMNs) and spinal motor neurons (SC MNs) express similar mRNA levels of glutamate ionotropic receptor AMPA, NMDA and kainate type subunits. The heatmap shows log2 RPKM values of these subunits and no separate clustering of the two cell types is observed. (b-c) Immunohistochemistry performed on generated OMNs and SC MNs at D1 in vitro in control conditions; similar levels of glutamate ionotropic receptor kainite type subunit 5 (Grik5) are found in both cell types. Scale bar in d 60 µm. (d-e) Microphotographs presenting SC MN and OMN response to kainic acid induced toxicity (20 µM) for a week. Scale bars in f = 100 µm. (f) Curves represent percentages of MN survival over time in OMN and SC MN cultures. OMNs were visualized as NF200+Islet1+Hb9- cells, while SC MNs as NF200+Islet1+Hb9+ cells. OMNs show increased survival to KA toxicity at D7 (mean ± SEM, 2way ANOVA and Tukey's multiple comparison test, F(9, 56)=2.333, *P =0.0261, SC MNs n=4; OMNs n=5) when compared to SC MNs (experiments were performed at least in quadruplicates, with technical replicates and with at least 130 motor neurons counted per condition in each experiment). (g-j) Sholl analysis was performed on OMN at D7 survival assay in control and KA20 conditions to assess individual MN arborization complexity during toxicity. Scale bar = 100 µm. (h) Sholl mask was applied to individual OMNs after specifying the radius from the center of the soma of the neuron and created concentric circles every 25 µm of increasing radius. (i) Comparison of average number of neurite intersections of OMN in control and KA20 toxicity conditions with radial step size of 25 µm. OMNs did not show reduction in arborization (multiple t test, n = 10 per condition). (j) Schematic depicting identification of neurite segments by Sholl analysis. Color code is assigned depending on arbor localization from the soma in an inside-out manner following the given radius. Multiple intersections within the same segment display the same colour.

Figure 3. Oculomotor neurons have high levels of Akt signaling. (a) Log10-transformed data obtained by DEG analysis shows preferential expression of Akt1 and Akt3 transcripts in the generated OMNs (adjusted *P < 0.05). (b) Graph shows differential expression of AKT1 and AKT3 transcripts in human OMNs and SC MNs isolated by LCM-seq, with both transcripts being preferential to OMNs (adjusted *P < 0.05). (c-d) Microphotographs show pAkt levels in OMN and SC MN cultures at D7 toxicity assay assessed by immunohistochemistry, pAKT staining alone in small inserts (red channel). (e) Fluorescense intensities, analyzed in a semi-quantitative manner, indicate higher expression of pAkt in OMNs (mean ± SEM, 2way ANOVA and Tukey's multiple comparison test , $F(1, 353)=66.1$, *** $P < 0.0001$, n=4). (f-g) β-catenin expression is maintained in OMN also during kainate toxicity. Scale bar = 60 µm. (h) Semi-quantitative analysis of β-catenin over NF200 staining intensities in OMNs and SC MNs in kainate conditions (mean ± SEM, t test, $t=6.799$ $df=69$, *** $P < 0.0001$, n=3). Scale bars = 60 µm.

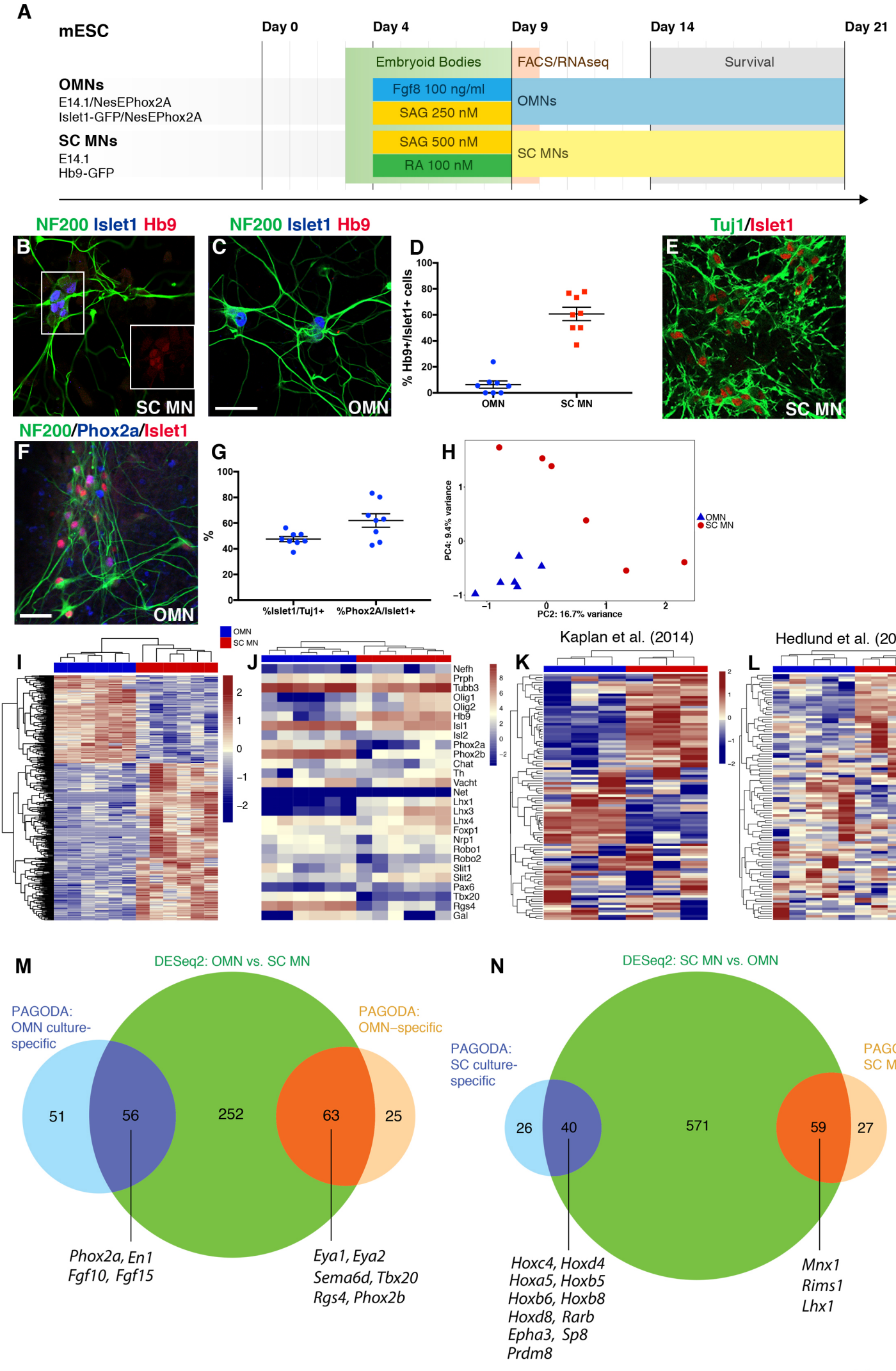

Figure 1

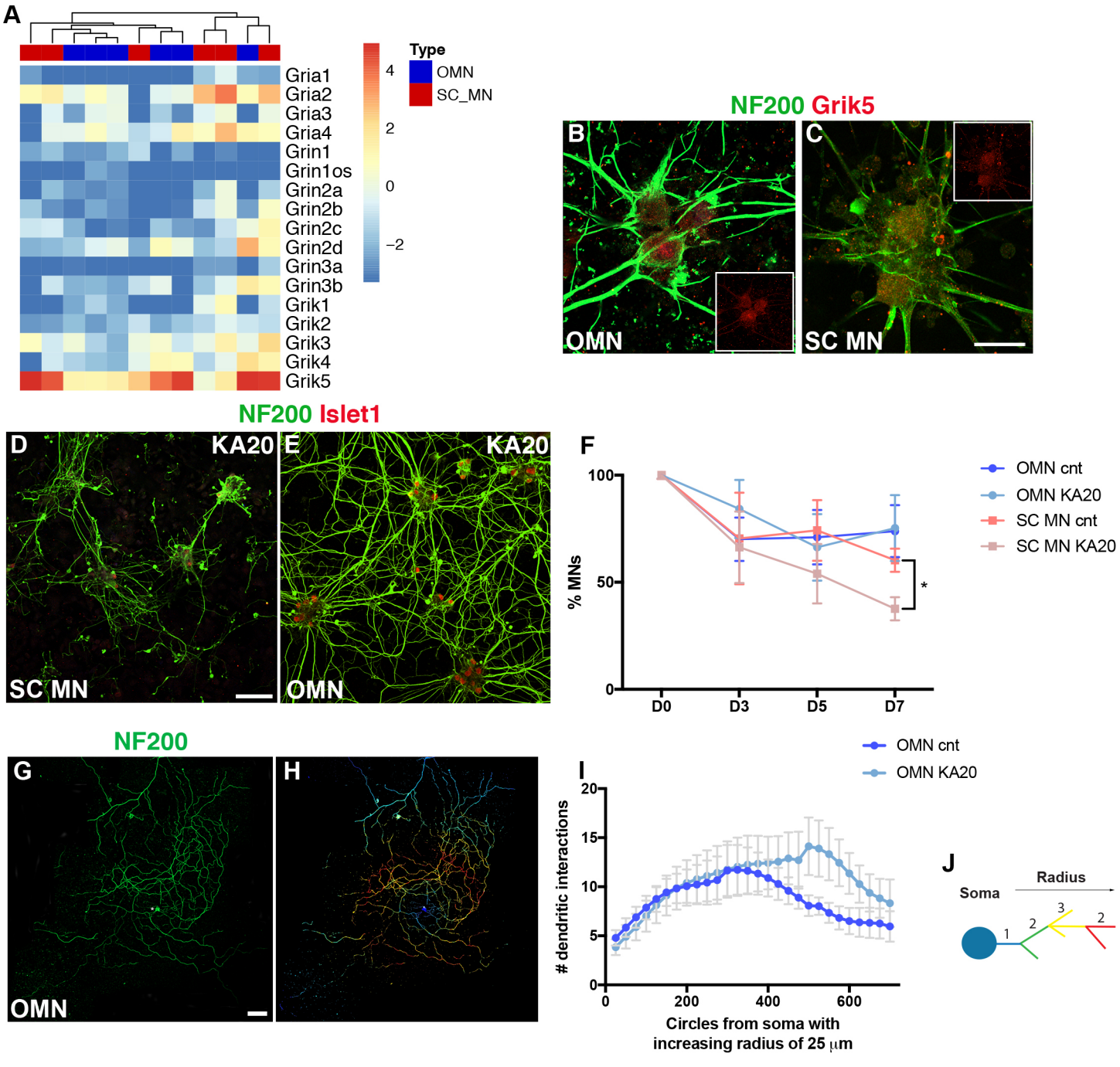
A
Type
OMN
SC_MN
4
2
0
−2
Gria1
Gria2
Gria3
Gria4
Grin1
Grin1os
Grin2a
Grin2b
Grin2c
Grin2d
Grin3a
Grin3b
Grik1
Grik2
Grik3
Grik4
Grik5
NF200 Grik5
B
OMN
C
SC MN
NF200 Islet1
D
KA20
SC MN
E
KA20
OMN
F
100
50
0
% MNs
D0
D3
D5
D7
*
OMN cnt
OMN KA20
SC MN cnt
SC MN KA20
NF200
G
OMN
H
I
OMN cnt
OMN KA20
20
15
10
5
0
dendritic interactions
0
200
400
600
Circles from soma with
increasing radius of 25 μm
J
Soma
Radius
1
2
3
2

Figure 2

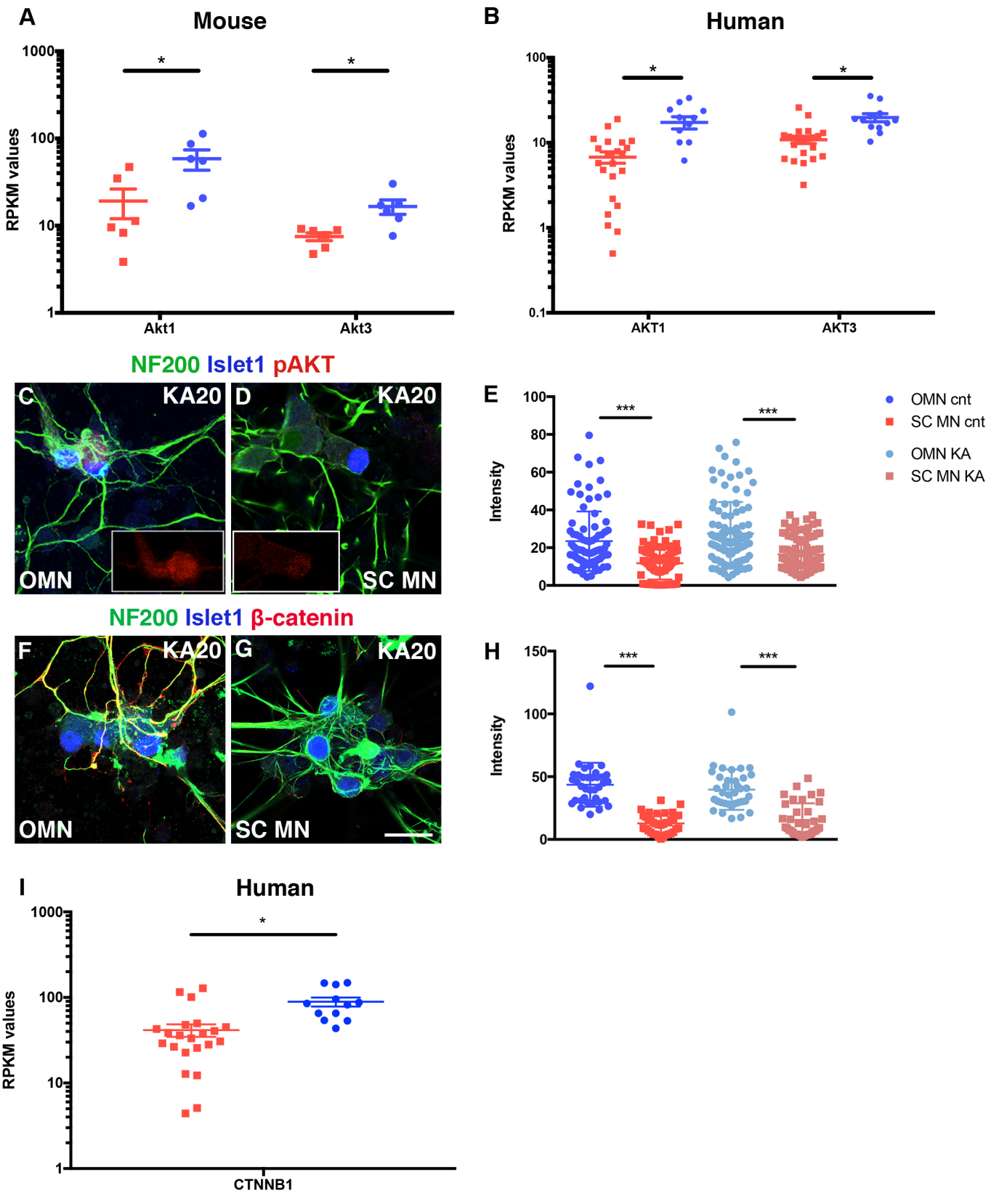
A
Mouse
RPKM values
1000
100
10
1
*
*
Akt1
Akt3
B
Human
RPKM values
100
10
1
0.1
*
*
AKT1
AKT3
NF200 Islet1 pAKT
C
KA20
OMN
D
KA20
SC MN
E
Intensity
100
80
60
40
20
0
***
***
OMN cnt
SC MN cnt
OMN KA
SC MN KA
NF200 Islet1 β-catenin
F
KA20
OMN
G
KA20
SC MN
H
Intensity
150
100
50
0
***
***
I
Human
RPKM values
1000
100
10
1
*
CTNNB1

Figure 3